

Py-GC/MS study of lignin pyrolysis and effect of catalysts on product distribution

Si Zhan^{1,2,3}, Wang Chenguang^{2*}, Bi Kang^{2,4}, Zhang Xinghua², Yu Chiling⁵,
Dong Renjie^{1,3,6*}, Ma Longlong², Pang Changle⁷

(1. Bioenergy and Environment Science & Technology Laboratory, College of Engineering, China Agricultural University, Beijing 100083, China; 2. Key Laboratory of Renewable Energy, Guangzhou Institute of Energy Conversion, Chinese Academy of Sciences, Guangzhou 510640, China; 3. Key Laboratory of Clean Production and Utilization of Renewable Energy, Ministry of Agriculture, Beijing 100083, China; 4. School of Chemical Engineering and Energy, Zhengzhou University, Zhengzhou 450001, China; 5. State Key Laboratory of Organic Geochemistry, Guangzhou Institute of Geochemistry, Chinese Academy of Sciences, Guangzhou 510640, China; 6. National Center for International Research of BioEnergy Science and Technology, Ministry of Science and Technology, Beijing 100083, China; 7. Department of Vehicle Engineering, College of Engineering, China Agricultural University, Beijing 100083, China)

Abstract: Fast pyrolysis is one of the most promising methods to convert lignin into fuels and chemicals. In the present study, pyrolysis-gas chromatography/mass spectrometry (Py-GC/MS) was used to evaluate vapor phase product distribution of lignin fast pyrolysis. During the non-catalytic pyrolysis process, lignin was pyrolyzed at 400°C, 500°C and 600°C respectively, finding that the highest yield of aromatic hydrocarbons was obtained at 600°C. Catalytic pyrolysis experiments were also conducted to investigate the effects of catalyst pore structure and acidity on the product distributions. Five different catalysts (HZSM-5, MCM-41, TiO₂, ZrO₂ and Mg(Al)O) were applied to lignin catalytic pyrolysis, and the catalytic performance was estimated by analyzing the pyrolytic products. The catalysts were characterized by using X-ray diffraction (XRD), BET, and NH₃ (CO₂) temperature programmed desorption. Based on these characterizations, discussion was carried out to explain the formation of the product distributions. Among the five catalysts, HZSM-5 exhibited the best performance on the formation of aromatic hydrocarbons.

Keywords: lignin, Py-GC/MS, fast pyrolysis, catalytic upgrading, pore structure, acid-base property

DOI: 10.25165/j.ijabe.20171005.2852

Citation: Si Z, Wang C G, Bi K, Zhang X H, Yu C L, Dong R J, et al. Py-GC/MS study of lignin pyrolysis and effect of catalysts on product distribution. *Int J Agric & Biol Eng*, 2017; 10(5): 214–225.

1 Introduction

Due to the depletion of fossil resources and concerns over carbon emission, lignocellulosic biomass has

emerged as a promising renewable feedstock for the production of fuels and chemicals. Pathways for biomass conversions can be categorized as biochemical or thermochemical processes. Fast pyrolysis of biomass and its three major components (i.e. cellulose,

Received date: 2016-09-13 **Accepted date:** 2017-06-14

Biographies: Si Zhan, PhD candidate, major in biomass catalytic conversion, Email: sizhan43@126.com; Bi Kang, Master, major in biomass catalytic conversion, Email: bikang@ms.giec.ac.cn; Zhang Xinghua, Associate professor, major in biomass catalytic conversion, Email: zhangxh@ms.giec.ac.cn; Yu Chiling, Senior Engineer, major in analytical test, Email: yuchiling@gig.ac.cn; Ma Longlong, Professor, major in biomass utilization and conversion, Email: mall@ms.giec.ac.cn. Pang Changle, Professor, major in vehicle engineering, Email: pangcl@cau.edu.cn.

***Corresponding author:** Wang Chenguang, Professor, major in biomass catalytic conversion, Guangzhou Institute of Energy Conversion, Chinese Academy of Sciences, No.2 Wushan Nengyuanlu, Tianhe District, Guangzhou 510640, China. Tel/Fax: +86-20-37029721, Email: wangcg@ms.giec.ac.cn.

Dong Renjie, Professor, major in biomass engineering, China Agricultural University, No. 17 Qinghua Donglu, Haidian District, Beijing 100083, China. Tel/Fax: +86-10-62737885, Email: rjdong@cau.edu.cn.

hemicelluloses and lignin) is a relatively simple thermochemical process which is usually conducted at a temperature of 400°C-600°C in the absence of oxygen^[1], and has the advantages of high conversion efficiency and environmentally friendly^[2]. One of the primary advantages of fast pyrolysis is that solid biomass can be directly converted to liquid fuels, i.e. pyrolysis oil. However, high oxygen content (20%-40%) of pyrolysis oil leads to undesirable properties such as low energy density, high viscosity and corrosion, thermal and chemical instability. Thus, catalytic upgrading was used to improve the qualities of pyrolysis oil. Catalytic pyrolysis was proved to be an effective way to improve the bio-oil quality. Aho et al.^[3] carried out catalytic pyrolysis of pine wood with H β , HY, HZSM-5 and Mordenite, finding that acids and alcohols were decreased in the presence of HZSM-5. Zhang et al.^[4] studied the effect of HZSM-5 on fast pyrolysis of corn cob in a fluidized bed, proposing that the existence of catalyst could decrease 25% oxygen content of pyrolysis oil, while increase the yields of gas, water and coke. On account of the complexities of pyrolysis process and productions, some researchers turned to investigate the catalytic pyrolysis of individual component of lignocellulosic biomass to further understand the pyrolysis mechanisms. Carlson et al.^[5] tested several catalysts including ZSM-5, silicalite, β , Y-zeolite and silica-alumina on the pyrolysis of cellulose and obtained the highest yield of aromatics in the presence of ZSM-5. Karanjkar et al.^[6] obtained a similar aromatic yield of 39.5% C from catalytic pyrolysis of cellulose using ZSM-5 as catalyst. Zhu et al.^[7] investigated the effect of HZSM-5 and M/HZSM-5 (M = Fe, Zn) on xylan pyrolysis, revealing that catalytic pyrolysis reduced oxygenates yield and increased hydrocarbons yield. Kim et al.^[8] presented that mesoporous Y zeolite with larger quantity and stronger acidity could also reduce the oxygenates content and increase the aromatics to a larger extent from xylan pyrolysis. Guo et al.^[9] found that USY catalyst performed the best effect on deoxygenation than HZSM-5 and H β in xylan pyrolysis.

A representative lignin structure showing three

primary units is illustrated in Figure 1^[10]. The difference with cellulose and hemicellulose, lignin is a cross-linked amorphous biopolymer of three primary units including guaiacol (G), syringyl (S) and *p*-hydroxyphenol (H) units which are bonded with C-O-C and C-C bonds^[11]. Additionally, the content of each unit is varied with plant types. For example, conifer wood (softwood) contains 90%-95% G unit, 0-1% S unit and 0.5%-3.4% H unit^[12]. The aromatic rings existed in the primary units are conducive to the immediate conversion of lignin to aromatic products^[13]. However, the wide distribution of lignin pyrolysis productions caused by the complex structure^[14,15] results in receiving relatively less attention compared to cellulose and hemicellulose. Hence, the understanding of pyrolysis process and the effect of catalyst is essential. Thring et al.^[16] investigated the effect of HZSM-5 in the catalytic pyrolysis of lignin in a fixed bed reactor and obtained the highest toluene yield (44 wt.%) at 650°C. The deactivation of zeolite catalyst during lignin pyrolysis was likely caused by simple phenols produced from the deconstruction of the lignin polymer^[17]. The role of shape selectivity in lignin pyrolysis was studied by Yu et al.^[18], suggesting that ZSM-5 produced the highest aromatic yield, while β zeolite was suited to convert bulky oxygenates. Adhikari et al.^[19] used four zeolite catalysts with different SiO₂/Al₂O₃ ratios to catalyze torrefied lignin pyrolysis, and as high as 35 wt.% carbon yield of aromatic hydrocarbons was obtained in the presence of the zeolite with SiO₂/Al₂O₃=30. Extensive researches focused on the zeolite catalysts and the effect of acidic sites on the pyrolysis of lignin. In comparison, less investigation focused on the catalytic pyrolysis over metal oxides with acidic/base property. In the present study, five catalysts with different properties including HZSM-5, MCM-41, TiO₂, ZrO₂ and Mg(Al)O were selected to investigate the influences of pore size, acidic and base properties on lignin pyrolysis. The experiments were conducted by using a Py-GC/MS system and the yield and product distribution were systematically studied to reveal the effects of different catalysts.

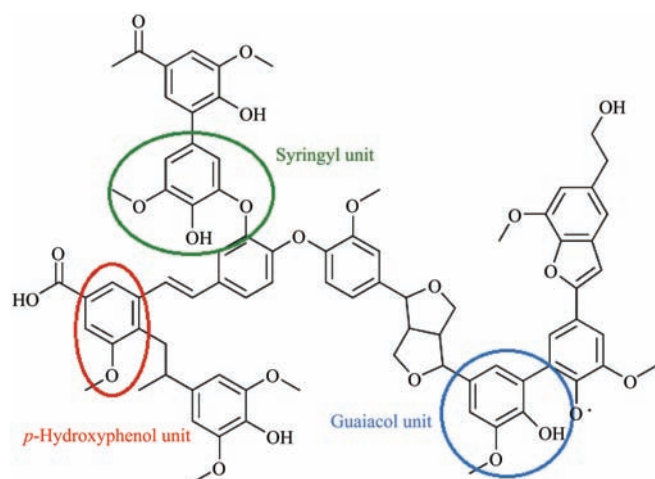


Figure 1 Representative structure models of lignin. Adapted from Kloekhorst et al.^[10]

2 Experimental materials and layout

2.1 Materials

Lignin used in this study was a Kraft lignin from softwood obtained from Mead Westvaco Co. (USA). Commercial zeolites HZSM-5 (Si/Al=38) and MCM-41 were purchased from Nankai University Catalyst Co., Ltd; ZrO₂ and TiO₂ were purchased from Aladdin; The MgAlO (Mg/Al molar ratio = 2:1) catalyst was prepared in the following manner: solution A was prepared by dissolving 10.0 g Mg(NO₃)₂·6H₂O and 7.76 g Al(NO₃)₃·9H₂O in 50 mL of deionized water; solution B was prepared by dissolving 3.82 g NaOH and 4.38 g Na₂CO₃ in 50 mL of deionized water. Solutions A and B were simultaneously added dropwise to 50 mL of deionized water with constant stirring at 100°C for 12 h. After that, the slurry was filtered, completely rinsed with distilled water and dried at 100°C for 8 h. Finally, the dried product was calcined at 550°C in air for 5 h with a heating rate of 5°C/min. Mg(NO₃)₂·6H₂O, Al(NO₃)₃·9H₂O, NaOH and Na₂CO₃ used here were analytical grade and obtained from Aladdin Reagent Co., Ltd (Shanghai, China). Lignin and catalysts were all dried at 80°C for 12 h before use.

2.2 Characterization

FT-IR spectra were obtained on a Nicolet iS50 FT-IR spectrophotometer (Thermo Scientific, USA). A mercury cadmium telluride (MCT) detector was used and the spectrum was recorded in the range of 4000-500 cm⁻¹. Elemental analysis were performed by a vario EL cube elemental analyzer (Elementary, Germany) which

reported the composition of lignin in weight percentage of carbon, hydrogen, nitrogen and sulfur. The content of oxygen was calculated by difference.

The crystallographic properties of the catalysts were characterized on an X-ray diffractometer (X'pert PRO, Panalytical, Netherlands) with a CuKα (λ=0.154 nm) radiation source operated at 40 kV and 100 mA. The 2θ ranged from 5° to 80° with 0.02° step size.

The textural properties of catalysts were determined by N₂ (or Ar for HZSM-5) isothermal adsorption using a QUADRASORB SI analyzer equipped with QuadraWin software system. Prior to analysis, all samples were degassed at 300°C for 8 h. The surface area was analyzed by the Brunauer-Emmett-Teller (BET) method and the pore size distribution was calculated by Density Functional Theory (DFT) method.

The density and strength of acid sites of catalysts were determined by NH₃ temperature-programmed desorption (NH₃-TPD). The sample (200 mg) was firstly pre-treated at 400°C for 60 min in Helium, then cooled to 30°C and exposed to a 10% NH₃/He stream for 60 min. The desorption of NH₃ was carried out by flushing with He by increasing the temperature to 850°C at the heating rate of 10°C/min.

The basic characteristics of the Mg(Al)O catalyst was studied with CO₂-temperature programmed desorption (CO₂-TPD). The sample (200 mg) was pretreated at 400°C for 60 min in He, followed by cooling to 80°C under He flow and subsequent exposed to a 40% CO₂/He stream for 60 min. Flushing with He at 80°C for 3 h was applied to remove the adsorbed CO₂, and TPD analysis was carried out from 80°C to 600°C at a heating rate of 10°C/min.

2.3 Py-GC/MS system

Pyrolysis experiments were conducted using in a micro-furnace single shot pyrolyzer (PY-2020iD, Frontier Laboratories, Japan) equipped with an auto-sampler (AS-1020E, Frontier Laboratories, Japan). For catalytic pyrolysis experiments, about 6 mg of lignin was firstly introduced into a deactivated stainless steel sample cup, over which 6 mg of the catalyst was put. For non-catalytic experiments, only 6 mg of lignin was loaded. Subsequently, a little amount of quartz wool

was loaded above the sample layer for each experiment to avoid powder spraying caused by carrier gas. The sample cup was then dropped into the pre-heated furnace under a flow of He as carrier gas.

Pyrolysis was performed for 1 min, and the pyrolysis vapor was analyzed by a Thermo Ultra-Trace gas chromatograph (GC) with a Thermo DSQ II Mass spectrometer (MS) connected to the pyrolyzer. Chromatographic separation of the pyrolysis products was done with a (5%-phenyl)-methylpolysiloxane non-polar column (HP-5MS, 60 m×0.25 mm×0.25 μm, Agilent Technologies, USA) with a carrier gas flow of 1.5 mL/min. The injector temperature was 280°C and a split ratio 1:40 were used. The GC oven was held at 40°C for 3 min and then heated to 300°C at 5°C/min with a dwell time of 20 min. The interface temperature between GC and MS was 280°C, and the ion source temperature was 230°C. Mass spectra were recorded under electron ionization (70 eV) at the mass range from 45 m/z to 300 m/z, using a scan rate of 1.0 s/decade. Identification of the pyrolysis compounds was carried out by comparison of their mass fragment with the National Institute of Standards and Technology (NIST) mass spectral library. Since the chromatographic peak area of a compound is considered linear with its quantity, a semi-quantitative estimation was used in this study that the yield and content of compounds could be revealed by peak area and peak area%, respectively.

3 Results and discussion

3.1 Characterization of lignin

Lignin structure could directly affect pyrolysis product distribution, so that FT-IR was firstly used to investigate the bond structure of lignin. The FT-IR spectrum result is shown in Figure 2 and the corresponding assignments of bonds are given in Table 1 according to previous researches. The broad band around 3415 cm⁻¹ was caused by O-H stretching vibration. The bond at 2930 cm⁻¹ and 1454 cm⁻¹ were assigned respectively to C-H stretching vibration and C-H bending vibration attributable to the methyl and methylene groups. The peak at 1130 cm⁻¹ had lower intensity than that at 1270 cm⁻¹ indicating lower syringyl (S) unit content.

Moreover, strong signals at 1515 cm⁻¹ and 1032 cm⁻¹ also indicated a predominance of guaiacol (G) units in this lignin, consisting with the C-H out-of-plane deformation bands at 854 cm⁻¹ and 817 cm⁻¹ typical of G rings. FT-IR results suggested that the lignin used here was mainly composed of G type rings.

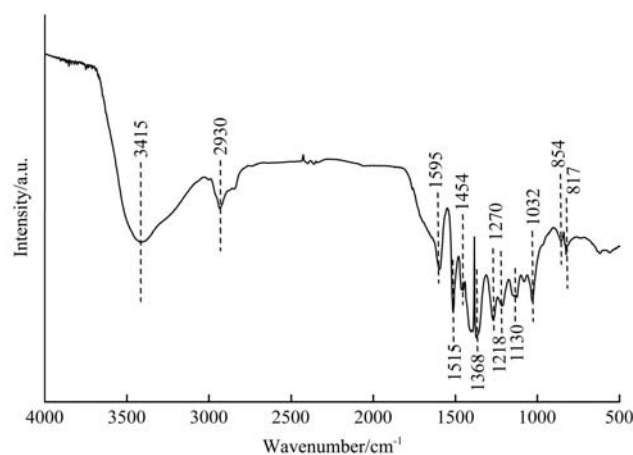


Figure 2 FT-IR spectrum of lignin

Table 1 Assignment of FT-IR spectrum of lignin

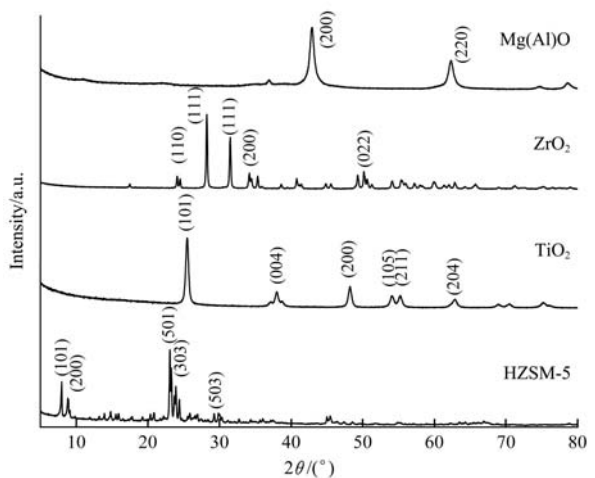
Peak/cm ⁻¹	Assignment	<i>Miscanthus</i> Lignin ^[20] /cm ⁻¹	Flax shives ^[21] /cm ⁻¹
3415	O-H stretching	3435	3398
2930	C-H stretching in -CH ₃ and -CH ₂ -	2981	2933, 2848
1595	Aromatic skeletal vibrations (S>G)	1603	1593
1515	Aromatic skeletal vibrations (G>S)	1508	1508
1454	C-H bending in -CH ₃ and -CH ₂ -	1463	1462
1368	Aliphatic C-H stretching in CH ₃ , not in OMe	1366	1369
1270	Guaiacol ring breathing	1267	1265
1218	C-O stretch	1230	1217
1130	Syringyl ring breathing	1126	1122
1032	Aromatic C-H in plane deformation (G>S)	1034	1030
854, 817	Aromatic C-H out-of-plane deformation (G)	-	854, 816

Note: Peak assignments from *Miscanthus* lignin and flax shives are presented for comparison.

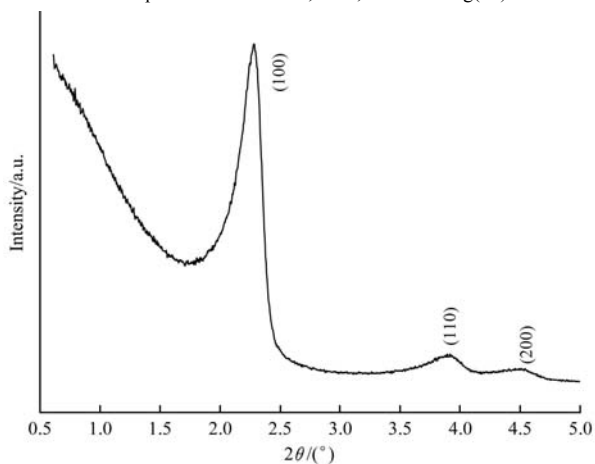
3.2 Characterization of catalysts

Since the crystal structure of catalysts played a role on the catalytic pyrolysis process of lignin^[14], XRD patterns of five catalysts used in this study are shown in Figure 3. The crystal structures of these five catalysts were significantly different from each other. The diffraction peaks in HZSM-5 were mainly at 2θ=7.4°-9.3° and 22.5°-24.8°. HZSM-5 had a typical diffraction pattern assigned to the MFI orthorhombic structure which consists of two channels of 10-membered rings and zigzag channels^[22]. The pattern of TiO₂ exhibited

strong peaks at $2\theta=24^\circ$ and 48° corresponding to the anatase phase with tetragonal system^[23]. The peaks were in good agreement with the standard spectrum (JCPDS NO.: 21-1272). The diffraction peaks in ZrO_2 pattern were mainly at $2\theta=24.0^\circ$, 28.2° , 31.5° , 34.1° and 50.0° (JCPDS NO.: 37-1484), which exhibited monoclinic phase while no tetragonal phase was observed^[24]. The XRD pattern of $Mg(Al)O$ exhibited the typical features of a mixed oxide of $Mg(Al)O$ type. peaks at $2\theta=42.8^\circ$ and 62.2° corresponded to a periclase MgO or rather magnesia-alumina solid solution, while no obvious peaks of Al_2O_3 phase appeared suggesting Al^{3+} cations were well dispersed in the structure of MgO without formation of spinel species^[25]. The XRD pattern of MCM-41 in Figure 3b exhibited a characteristic intense (100) peak at $2\theta=2.25^\circ$ and two higher order (110) and (200) reflections at $2\theta=3.95^\circ$ and 4.60° , which could be indexed to the $p6m$ space group, indicating a hexagonal mesostructure^[26,27].



a. XRD patterns of HZSM-5, TiO_2 , ZrO_2 and $Mg(Al)O$



b. XRD patterns of MCM-41

Figure 3 XRD patterns of HZSM-5, TiO_2 , ZrO_2 , $Mg(Al)O$ and MCM-41

Figure 4 shows the NH_3 -TPD results of five catalysts. The peaks appeared at $210^\circ C$ - $240^\circ C$ were corresponded to the desorption of ammonia from the weak acid sites and the peaks at $434^\circ C$ - $590^\circ C$ were assigned to the strong acid sites in the characterization of HZSM-5 and $Mg(Al)O$. TiO_2 also showed strong acid sites around $382^\circ C$ and $561^\circ C$, while the peak intensity was weak, indicating the relatively low amounts of acid sites. MCM-41 and ZrO_2 showed no obvious peaks of TPD curves, indicating that these catalysts had very weak acid sites. The peak areas representing the amount of acid sites are summarized in Table 2. It is found that the total peak area of HZSM-5 was the largest among the five catalysts, while that of ZrO_2 was the smallest one. $Mg(Al)O$ was obtained by the thermal decomposition of hydrotalcites, which showed pairs of acid and basic sites. These pairs of acid and basic sites were obtained by the insertion of Al in the MgO lattice or the presence of Mg in the $\gamma-Al_2O_3$ lattice^[28]. Accordingly, the basicity of $Mg(Al)O$ was measured by CO_2 -TPD. As shown in Figure 5, three peaks were observed, two of which appeared at $195^\circ C$ - $281^\circ C$ assigned to relatively weak basic sites and the other one at about $494^\circ C$ assigned to strong basic sites.

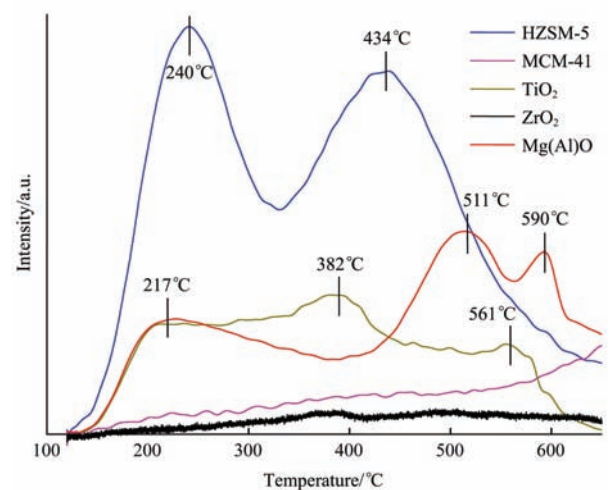
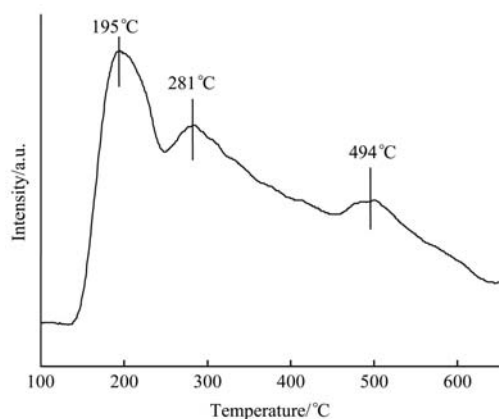


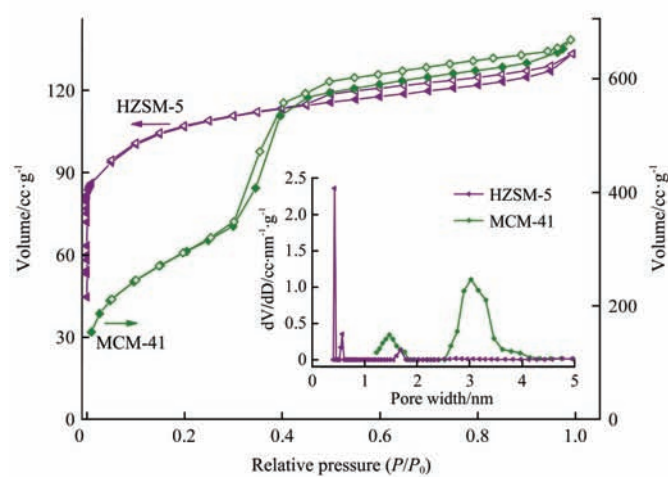
Figure 4 NH_3 -TPD profile of five catalysts used in this study

Table 2 Physical-chemical properties of the catalysts

Catalysts	BET surface area / $m^2 \cdot g^{-1}$	Total pore volume / $cm^3 \cdot g^{-1}$	Total peak area of NH_3 -TPD
HZSM-5	393.514	0.21	3486
MCM-41	1067.66	1.03	524
TiO_2	71.83	0.44	1285
ZrO_2	5.49	0.03	200
$MgAlO$	126.74	0.58	1666

Figure 5 CO₂-TPD profile of Mg(Al)O catalyst

The porosity of the five catalysts is illustrated in Figure 6, and the surface area and total pore volume are



a. HZSM-5 and MCM-41

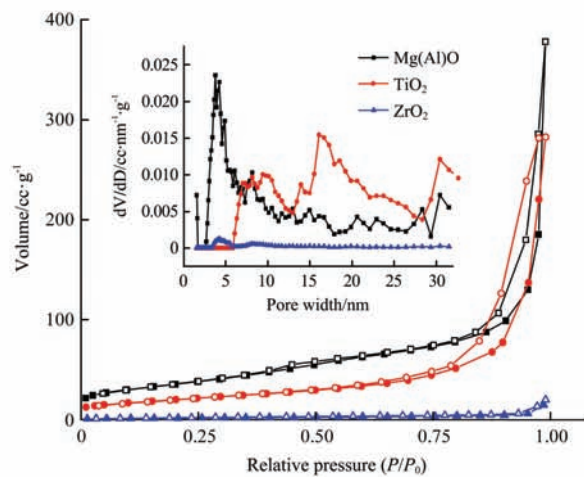
b. ZrO₂, TiO₂ and Mg(Al)O

Figure 6 Adsorption/desorption isotherms and pore size distribution of studied catalysts

3.3 Effect of temperature on lignin pyrolysis

The products of lignin fast pyrolysis included non-condensable gas, volatile compounds and non-volatile oligomers. In the present py-GC/MS system, only volatile compounds could be analyzed, and the identified compounds were categorized into five categories: aromatic hydrocarbons, phenol-type compounds (phenols), catechol-type compound (catechols), alkoxy-type compounds (alkoxy) and polyaromatics. Alkoxy-type compounds were composed of guaiacol-type compounds and aromatic hydrocarbon alkoxy. Large molecular weight like sterols and non-identified compounds were classified as others. In order to know the connection between lignin structure and pyrolysis products, lignin was firstly pyrolyzed at different temperatures without catalyst. The product distribution for non-catalytic pyrolysis of

lignin at 400°C, 500°C and 600°C is shown in Table 3 and Figure 7. It is found that the total peak area increased significantly from 3.66×10^9 at 400°C to 1.68×10^{10} at 500°C and then slightly decreased to 1.45×10^{10} at 600°C with the increased pyrolysis temperature, indicating that high temperature was beneficial to increasing the yield of volatile liquid. Similar observation was made by Latridis et al.^[29] Lignin pyrolysis happened in a wide temperature range which started around 160°C. Linkages between the lignin units like α -O-4 were first cleaved between 200°C and 400°C due to the relatively low bond dissociation energy, which produced the alkoxy (e.g. guaiacol, 4-methyl-guaiacol, and vanillin) as the major products. With the increase of temperature, the amount of alkoxy increased obviously from 2.31×10^9 to 1.02×10^{10} . Due to the lignin used in this study was softwood lignin, the alkoxy obtained

listed in Table 2. Among the five catalysts, only HZSM-5 showed a dominant peak at 0.43 nm and another peak at 0.58 nm, indicating a microporous structure. MCM-41 showed a pore size distribution mainly centered at 3.04 nm corresponding to mesoporous structure. MCM-41 had the largest BET surface area and total pore volume among the five zeolite catalysts ($1067.66 \text{ m}^2/\text{g}$ for surface area and $1.03 \text{ m}^3/\text{g}$ for total pore volume). Both TiO₂ and Mg(Al)O showed a board pore size distribution ranged from 3.5 nm to 32 nm, indicating the existing of irregular mesoporous structure. ZrO₂ presented a non-porous characteristic with a BET surface area of only $5.49 \text{ m}^2/\text{g}$.

were mainly the G types, in accordance with the results of FT-IR. The aromatic hydrocarbons were only detected at 600°C, while its amount (peak area: 2.53×10^7) was relatively low. Furthermore, pyrolysis products became more complicated at relatively high temperatures due to more complicated depolymerization process and secondary reactions. The amount of 1,2-Benzenediol was found to be increased from 0 to 1.40×10^8 with the temperature elevated from 400°C to 600°C, while the amount of 3-methyl-1,2-Benzenediol increased from 0 to 9.02×10^7 . It could be attributed to that secondary decomposition occurred at high temperatures resulting in

the conversion of guaiacols into catechols^[30].

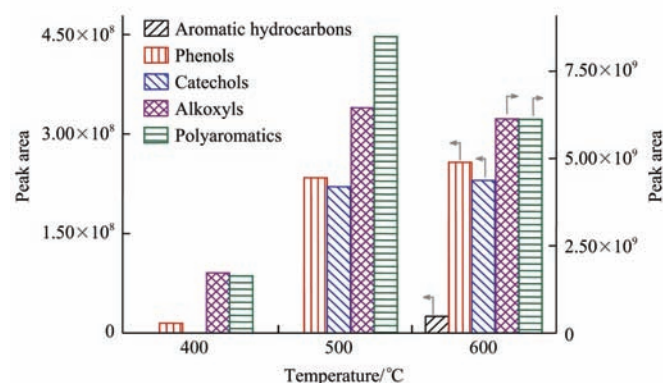
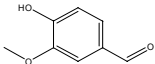
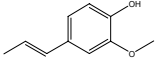
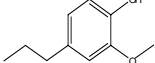
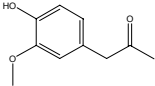
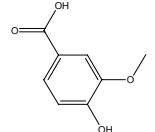
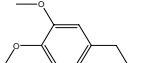
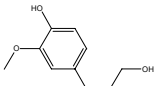
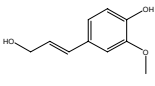


Figure 7 Effect of temperatures on the production distributions

Table 3 Product distribution for non-catalytic pyrolysis of lignin at different temperatures

Compounds	Structure	400/°C		500/°C		600/°C	
		Absolution peak area	Relative peak area/%	Absolution peak area	Relative peak area/%	Absolution peak area	Relative peak area/%
Toluene		0	0	0	0	2.53×10^7	0.17
Phenol		0	0	5.89×10^7	0.35	5.45×10^7	0.38
Methylphenol		1.51×10^7	0.41	1.27×10^8	0.76	1.34×10^8	0.93
Dimethyl-phenol		0	0	4.77×10^7	0.28	6.84×10^7	0.47
1,2-Benzenediol		0	0	1.33×10^8	0.79	1.40×10^8	0.97
3-methyl-1,2-benzenediol		0	0	8.78×10^7	0.52	9.02×10^7	0.62
Guaiacol		3.35×10^8	9.16	9.17×10^8	5.46	6.68×10^8	4.62
2-methoxy-5-methylphenol		2.48×10^8	6.78	7.52×10^8	4.48	5.33×10^8	3.68
2,4-dimethoxytoluene		1.20×10^7	0.33	3.65×10^7	0.22	0	0
Phenol,4-ethyl-2-methoxy-		1.02×10^8	2.78	4.65×10^8	2.77	5.29×10^8	3.65
2-Methoxy-4-vinylphenol		2.48×10^8	6.77	6.84×10^8	4.08	5.15×10^8	3.56
Eugenol		3.72×10^7	1.02	6.75×10^8	4.02	4.62×10^8	3.19

Compounds	Structure	400/°C		500/°C		600/°C	
		Absolute peak area	Relative peak area/%	Absolute peak area	Relative peak area/%	Absolute peak area	Relative peak area/%
Vanillin		1.15×10^8	3.14	4.43×10^8	2.64	4.28×10^8	2.96
Phenol,2-methoxy-4-(1-propenyl)-		1.34×10^7	3.67	0	0	0	0
Phenol,2-methoxy-4-propyl-		2.09×10^7	0.57	0	0	0	0
2-Propanone,1-(4-hydroxy-3-methoxyphenyl)-		4.92×10^7	1.35	2.23×10^8	1.33	2.36×10^8	1.63
Vanillic acid		0	0	0	0	1.68×10^8	1.16
Benzene,1,2-dimethoxy-4-propyl-		2.64×10^7	0.72	1.49×10^8	0.89	1.79×10^8	1.23
Benzenepropanol,4-hydroxy-3-methoxy-		1.45×10^7	3.96	7.19×10^8	4.29	9.60×10^8	6.63
Phenol,4-(3-hydroxy-1-propenyl)-2-methoxy-		1.79×10^8	4.90	1.10×10^9	6.56	1.13×10^9	7.80
Polyaromatics	-	1.6×10^9	44.76	8.49×10^9	50.62	6.12×10^9	42.30
Others	-	1.6×10^8	4.41	1.38×10^9	8.23	1.70×10^9	11.77

3.4 Production distribution from catalytic pyrolysis of lignin

To investigate the performances of catalysts on the product distribution of lignin pyrolysis, catalytic pyrolysis of lignin with zeolites (HZSM-5, MCM-41) and metal oxides (TiO_2 , ZrO_2 , $\text{Mg}(\text{Al})\text{O}$) were conducted. Since the aromatic hydrocarbons were produced at 600°C, the catalytic pyrolysis was conducted at the same temperature. Table 4 and Figure 8 show the product distribution from catalytic pyrolysis of lignin with HZSM-5 and MCM-41. In the first column of the Table 4, non-catalytic pyrolysis is listed for comparison of the catalysts effect on the product distribution of the volatile liquid fraction. It is found that the total amount was both decreased with the two zeolite catalysts. In the presence of HZSM-5 catalysts, the amount of alkoxy decreased from 6.13×10^9 to 5.35×10^9 , and aromatic hydrocarbons significantly increased from 2.53×10^7 to 2.24×10^8 . Previous studies showed that HZSM-5 zeolite contained Bronsted acid sites that were favorable for the formation of aromatic hydrocarbons^[31-33]. Li et al.^[34]

also obtained similar results and demonstrated that as the acidity of HZSM-5 increased, the yields of aromatic hydrocarbons increased. In addition to acidity, pore structure could also affect the catalytic process significantly due to shape selectivity^[35]. However, most oxygenates derived from lignin pyrolysis had a larger dimension than the pore size of HZSM-5, resulting that oxygenates could only be converted at the external surface, in which only existed a small fraction of acid sites^[18]. This might be the reason for the relatively low yield of aromatic hydrocarbons with HZSM-5 in this study. Comparing with the non-catalytic pyrolysis, the peak area decreased obviously from 1.45×10^{10} to 3.65×10^9 , indicating the yield of volatile liquid fraction decreased with the use of MCM-41. Iliopoulou et al.^[36] observed polycyclic aromatic hydrocarbons (PAHs) and heavy compounds were significantly increased with MCM-41 as catalyst, compared to the non-catalytic experiment, due to its high thermal cracking activity. But it could not be able to further convert these heavy compounds to

hydrocarbons due to the lack of acid site. In our study, polyaromatics were not detected resulting in the decrease of volatile liquid yield. This might be

attributed to the further polymerization of heavy fraction resulting in the formation of non-volatile oligomers, which could not be detected in our system.

Table 4 Product distribution for pyrolysis of lignin with different zeolites at 600°C

Compounds	Non-catalytic		HZSM-5		MCM-41	
	Peak area	Peak area/%	Peak area	Peak area/%	Peak area	Peak area/%
Toluene	2.53×10^7	0.17	1.10×10^8	0.89	4.34×10^7	1.19
m-Xylene	0	0	1.13×10^8	0.91	0	0
Ethylbenzene	0	0	0	0	1.75×10^7	0.48
Phenol	5.45×10^7	0.38	1.18×10^8	0.94	1.06×10^8	2.91
Methylphenol	1.34×10^8	0.93	2.00×10^8	1.60	2.55×10^8	6.99
Dimethyl-phenol	6.84×10^7	0.47	1.33×10^8	1.07	1.24×10^8	3.40
Phenol,4-ethyl-	0	0	0	0	4.07×10^7	1.11
1,2-Benzenediol	1.40×10^8	0.97	0	0	0	0
3-methyl-1,2-benzenediol	9.02×10^7	0.62	1.56×10^8	1.25	0	0
Guaiacol	6.68×10^8	4.62	5.61×10^8	4.50	7.82×10^8	21.40
3-ethoxy-phenol	0	0	0	0	2.68×10^7	0.73
2-methoxy-5-methylphenol	5.33×10^8	3.68	8.35×10^8	6.70	5.51×10^8	15.09
2,4-dimethoxytoluene	0	0	0	0	5.06×10^7	1.38
Phenol,4-ethyl-2-methoxy-	5.29×10^8	3.65	5.55×10^8	4.45	3.20×10^8	8.75
2-Methoxy-4-vinylphenol	5.15×10^8	3.56	6.25×10^8	5.01	2.50×10^8	6.83
Eugenol	4.62×10^8	3.19	6.77×10^8	5.43	2.78×10^8	7.61
Vanilin	4.28×10^8	2.96	4.22×10^8	3.38	2.12×10^8	5.80
Phenol,2-methoxy-4-propyl-	0	0	0	0	5.37×10^7	1.47
Ethanone,1-(4-hydroxy-3-methoxyphenyl)-	3.28×10^8	2.27	3.82×10^8	3.06	1.71×10^8	4.69
2-Propanone,1-(4-hydroxy-3-methoxyphenyl)-	2.36×10^8	1.63	1.86×10^8	1.49	4.95×10^7	1.35
Vanillic acid	1.68×10^8	1.16	1.30×10^8	1.05	0	0
Benzene,1,2-dimethoxy-4-propyl-	1.79×10^8	1.23	1.28×10^8	1.03	0	0
Benzenepropanol,4-hydroxy-3-methoxy-	9.60×10^8	6.63	5.12×10^8	4.11	0	0
Phenol,4-(3-hydroxy-1-propenyl)-2-methoxy-	1.13×10^9	7.80	3.43×10^8	2.76	0	0
Polyaromatics	6.12×10^9	42.30	5.12×10^9	41.07	0	0
Others	1.70×10^9	11.77	1.16×10^9	9.31	3.22×10^8	8.82

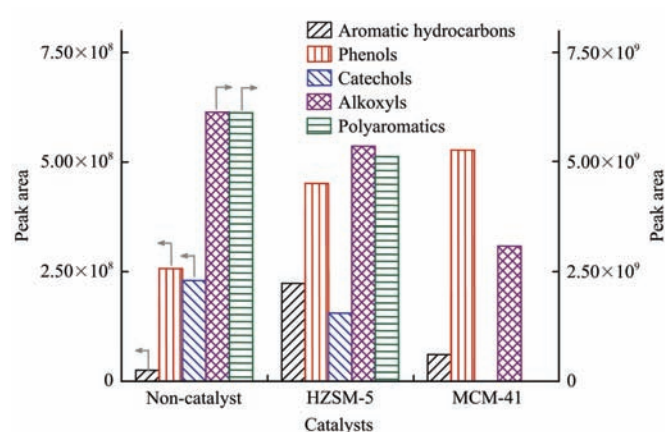


Figure 8 Effect of the zeolite catalysts on the production distributions

Table 5 and Figure 9 show the product distribution from catalytic pyrolysis of lignin with TiO_2 , ZrO_2 and $\text{Mg}(\text{Al})\text{O}$. In the presence of TiO_2 , the amount of aromatic hydrocarbons increased from 2.53×10^7 to 6.55×10^7 and phenols increased from 2.57×10^8 to

1.24×10^9 . The highest amount of phenol-type compounds was achieved with the use of TiO_2 . This might be attributed to the complete and incomplete deoxygenation of alkoxylys, since the amount of alkoxylys decreased from 6.13×10^9 to 3.87×10^9 . The highest alkoxylys yield was obtained in the presence of ZrO_2 , while the aromatic hydrocarbon yield was barely changed. Due to the much lower surface area, ZrO_2 could lead to high yield of oxygenates and be less effective on deoxygenation than TiO_2 ^[37]. This result was similar to Kaewpengkrow et al.^[38] who studied the effect of catalyst supporters including Al_2O_3 , ZrO_2 , TiO_2 (rutile) and TiO_2 (anatase) on upgrading the pyrolysis vapors, and found that the yield of aromatic hydrocarbons of TiO_2 (anatase) was higher than ZrO_2 and TiO_2 (rutile). Pyrolysis with acidic catalysts was prone to form coke via oligomerization, so that catalysts owing basic sites were

expected to reduce coke formation during pyrolysis process. Mg(Al)O catalyst with both acidic and base sites was selected in comparison to acidic catalyst. The amount of aromatic hydrocarbons increased from 2.53×10^7 to 5.09×10^7 . However, the Mg(Al)O catalyst resulted in an obvious reduction in the yield of volatile liquid fraction. The peak area of alkoxylys sharply decreased from 6.13×10^9 to 1.34×10^9 , and that of

polyaromatics also decreased from 6.12×10^9 to 9.65×10^8 . Auta et al.^[39] also obtained the similar results with MgO catalyst that the yields of liquid decreased while the yields of gas and char increased. Wang et al.^[40] also investigated the catalytic pyrolysis with base catalyst (CaO). The residue yield was much higher than the non-catalytic run at 600°C , which meant to the lower yield of liquid products.

Table 5 Product distribution for pyrolysis of lignin with different metal oxides at 600°C

Compounds	Non-catalytic		TiO ₂		ZrO ₂		MgAlO	
	Peak area	Peak area/%						
Benzene	0	0	2.19×10^7	0.20	0	0	0	0
Toluene	2.53×10^7	0.17	3.54×10^7	0.32	2.32×10^7	0.13	3.72×10^7	1.05
m-Xylene	0	0	8.19×10^6	0.07	7.80×10^6	0.04	1.37×10^7	0.39
Phenol	5.45×10^7	0.38	2.60×10^8	2.32	8.90×10^7	0.50	7.74×10^7	2.18
Methylphenol	1.34×10^8	0.93	5.60×10^8	5.00	1.85×10^8	1.03	1.95×10^8	5.52
Dimethyl-phenol	6.84×10^7	0.47	2.03×10^8	1.81	7.70×10^7	0.43	1.49×10^8	4.20
Phenol,4-ethyl-	0	0	1.65×10^8	1.48	5.00×10^7	0.28	0	0
Phenol,3-ethyl-5-methyl-	0	0	5.20×10^7	0.46	0	0	0	0
1,2-Benzenediol	1.40×10^8	0.97	1.31×10^8	1.17	3.42×10^8	1.91	0	0
3-methyl-1,2-benzenediol	9.02×10^7	0.62	0	0	1.25×10^8	0.70	0	0
4-ethyl-1,3-benzenediol	0	0	9.02×10^7	0.81	4.76×10^7	0.27	0	0
Guaiacol	6.68×10^8	4.62	2.48×10^8	2.21	7.81×10^8	4.35	2.45×10^8	6.91
2-methoxy-5-methylphenol	5.33×10^8	3.68	3.06×10^8	2.73	8.41×10^8	4.69	3.22×10^8	9.08
2,4-dimethoxytoluene	0	0	0	0	3.40×10^7	0.19	4.10×10^7	1.16
Phenol,4-ethyl-2-methoxy-	5.29×10^8	3.65	4.04×10^8	3.60	6.41×10^8	3.57	1.63×10^8	4.60
2-Methoxy-4-vinylphenol	5.15×10^8	3.56	3.46×10^8	3.09	6.72×10^8	3.75	2.10×10^8	5.93
Eugenol	4.62×10^8	3.19	4.66×10^8	4.16	6.41×10^8	3.57	1.82×10^8	5.14
Vanilin	4.28×10^8	2.96	3.17×10^8	2.83	6.16×10^8	3.43	8.97×10^7	2.53
Ethanone,1-(4-hydroxy-3-methoxyphenyl)-	3.28×10^8	2.27	3.24×10^8	2.89	4.27×10^8	2.38	0	0
2-Propanone,1-(4-hydroxy-3-methoxyphenyl)-	2.36×10^8	1.63	2.47×10^8	2.20	3.30×10^8	1.84	3.05×10^7	0.86
Vanillic acid	1.68×10^8	1.16	0	0	2.09×10^8	1.16	0	0
Benzene,1,2-dimethoxy-4-propyl-	1.79×10^8	1.23	1.62×10^8	1.45	2.87×10^8	1.60	0	0
Benzenepropanol,4-hydroxy-3-methoxy-	9.60×10^8	6.63	7.62×10^8	6.80	1.18×10^9	6.58	0	0
Phenol,4-(3-hydroxy-1-propenyl)-2-methoxy-	1.13×10^9	7.80	2.86×10^8	2.56	1.24×10^9	6.93	6.00×10^7	1.69
Polyaromatics	6.12×10^9	42.30	2.80×10^9	24.97	7.5×10^9	41.67	9.6×10^8	27.23
Others	1.70×10^9	11.77	3.01×10^9	26.88	1.6×10^9	8.99	7.6×10^8	21.51

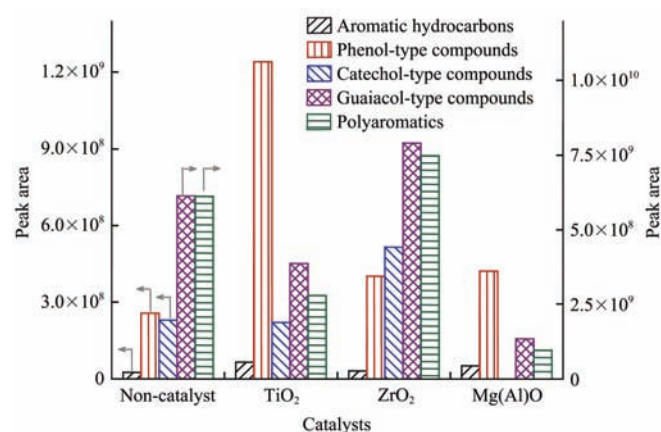


Figure 9 Effect of the metal oxides on the production distributions

4 Conclusion

Fast pyrolysis of lignin was carried out by py-GC/MS method to investigate the product distribution influenced by both temperature and catalyst. The predominant products of fast pyrolysis of lignin were alkoxylys, resulting from the cleavage of linkages between the lignin units like α -O-4. These alkoxylys products were mainly G type, which were in accordance with the lignin structure. For non-catalytic pyrolysis of lignin, the highest amount of volatile fraction was obtained at 500°C , while the highest amount of aromatic hydrocarbons was

obtained at 600°C. For catalytic pyrolysis of lignin, the amount of total volatile fraction changed in a wide range over catalysts with different structures and acid-base properties. The maximum production of aromatic hydrocarbons was achieved in the presence of HZSM-5, and the highest yield of liquid fraction was obtained in the addition of ZrO₂. The base catalyst, Mg(Al)O, led to the reduction of liquid yield by increasing the yield of oligomers and coke. Generally, the shape selectivity effect is in favor of the formation of aromatic hydrocarbons, but it has limited effect on the catalytic pyrolysis of lignin. Additionally, appropriate acid sites are needed for deoxygenation of oxygenates.

Acknowledge

This work was supported by The National Natural Science Foundation of China (51536009), NSFC (Natural Science Foundation of China) project (51476175), National Basic Research Program of China (2013CB228105), Chinese Academy of Sciences “one hundred talented plan”, and Beijing Municipal Key Discipline of Biomass Engineering.

[References]

- [1] Liaw S S, Perez V H, Zhou S, Rodriguez-Justo O, Garcia-Perez M. Py-GC/MS studies and principal component analysis to evaluate the impact of feedstock and temperature on the distribution of products during fast pyrolysis. *Journal of Analytical and Applied Pyrolysis*, 2014; 109: 140–151.
- [2] Anex R P, Aden A, Kazi F K, Fortman J, Swanson R M, Wright M M, et al. Techno-economic comparison of biomass-to-transportation fuels via pyrolysis, gasification, and biochemical pathways. *Fuel*, 2010; 89: S29–S35.
- [3] Aho A, Kumar N, Eränen K, Salmi T, Hupa M, Murzin D Y. Catalytic pyrolysis of woody biomass in a fluidized bed reactor: influence of the zeolite structure. *Fuel*, 2008; 87(12): 2493–2501.
- [4] Zhang H, Xiao R, Huang H, Xiao G. Comparison of non-catalytic and catalytic fast pyrolysis of corncob in a fluidized bed reactor. *Bioresource Technology*, 2009; 100(3): 1428–1434.
- [5] Carlson T R, Tompsett G A, Conner W C, Huber G W. Aromatic production from catalytic fast pyrolysis of biomass-derived feedstocks. *Topics in Catalysis*, 2009; 52(3): 241–252.
- [6] Karanjkar P U, Coolman R J, Huber G W, Blatnik M T, Almalkie S, Bruyn Kops S M, et al. Production of aromatics by catalytic fast pyrolysis of cellulose in a bubbling fluidized bed reactor. *AIChE Journal*, 2014; 60(4): 1320–1335.
- [7] Zhu X, Lu Q, Li W, Zhang D. Fast and catalytic pyrolysis of xylan: Effects of temperature and M/HZSM-5 (M=Fe, Zn) catalysts on pyrolytic products. *Frontiers of Energy and Power Engineering in China*, 2010; 4(3): 424–429.
- [8] Kim S S, Jun B R, Park S H, Jeon J K, Suh D J, Kim T W, et al. Catalytic upgrading of xylan over mesoporous y catalyst. *Journal of Nanoscience and Nanotechnology*, 2014; 14(4): 2925–2930.
- [9] Guo X, Wang S, Zhou Y, Luo Z. Catalytic pyrolysis of xylan-based hemicellulose over zeolites. *Int J Energy Environ*, 2011; 5(4): 137–142.
- [10] Kloekhorst A, Wildschut J, Heeres H J. Catalytic hydrotreatment of pyrolytic lignins to give alkylphenolics and aromatics using a supported Ru catalyst. *Catalysis Science & Technology*, 2014; 4(8): 2367–2677.
- [11] Okuda K, Umetsu M, Takami S, Adschiri T. Disassembly of lignin and chemical recovery-rapid depolymerization of lignin without char formation in water-phenol mixtures. *Fuel Processing Technology*, 2004; 85(8): 803–813.
- [12] Li C Z, Zhao X C, Wang A Q, Huber G W, Zhang T. Catalytic transformation of lignin for the production of chemicals and fuels. *Chemical Reviews*, 2015; 115(21): 11559–11624.
- [13] Neumann G T, Pimentel B R, Rensel D J, Hicks J C. Correlating lignin structure to aromatic products in the catalytic fast pyrolysis of lignin model compounds containing β-O-4 linkages. *Catalysis Science & Technology*, 2014; 4(11): 3953–3963.
- [14] Shen D, Zhao J, Xiao R, Gu S. Production of aromatic monomers from catalytic pyrolysis of black-liquor lignin. *Journal of Analytical and Applied Pyrolysis*, 2015; 111: 47–54.
- [15] Azadi P, Inderwildi O R, Farnood R, King D A. Liquid fuels, hydrogen and chemicals from lignin: A critical review. *Renewable and Sustainable Energy Reviews*, 2013; 21: 506–523.
- [16] Thring R W, Katikaneni S P, Bakhshi N N. The production of gasoline range hydrocarbons from Alcell® lignin using HZSM-5 catalyst. *Fuel Processing Technology*, 2000; 62(1): 17–30.
- [17] Mullen C A, Boateng A A. Catalytic pyrolysis-GC/MS of lignin from several sources. *Fuel Processing Technology*, 2010; 91(11): 1446–1458.
- [18] Yu Y, Li X, Su L, Zhang Y, Wang Y, Zhang H. The role of shape selectivity in catalytic fast pyrolysis of lignin with

- zeolite catalysts. *Applied Catalysis A: General*, 2012; 447: 115–123.
- [19] Adhikari S, Srinivasan V, Fasina O. Catalytic pyrolysis of raw and thermally treated lignin using different acidic zeolites. *Energy & Fuels*, 2014; 28(7): 4532–4538.
- [20] El Hage R, Brosse N, Chrusciel L, Sanchez C, Sannigrahi P, Ragauskas A. Characterization of milled wood lignin and ethanol organosolv lignin from miscanthus. *Polymer Degradation and Stability*, 2009; 94(10): 1632–1638.
- [21] Monteil-Rivera F, Phuong M, Ye M, Halasz A, Hawari J. Isolation and characterization of herbaceous lignins for applications in biomaterials. *Industrial Crops and Products*, 2013; 41: 356–364.
- [22] Kong X, Li X, Wu S, Zhang X, Liu J. Efficient conversion of cotton stalks over a Fe modified HZSM-5 catalyst under microwave irradiation. *RSC Advances*, 2016; 6(34): 28532–28537.
- [23] Liu S, Han L, Duan Y, Asahina S, Terasaki O, Cao Y, et al. Synthesis of chiral TiO₂ nanofibre with electron transition-based optical activity. *Nature communications*, 2012; 3: 1215.
- [24] Wang X X, Zhao J L, Hou X R, He Q, Tang C C. Catalytic activity of ZrO₂ nanotube arrays prepared by anodization method. *Journal of Nanomaterials*, 2012; 2012:1.
- [25] Xie W, Peng H, Chen L. Calcined Mg–Al hydrotalcites as solid base catalysts for methanolysis of soybean oil. *Journal of Molecular Catalysis A: Chemical*, 2006; 246(1): 24–32.
- [26] Bruzzoniti M C, Sarzanini C, Torchia A M, Teodoro M, Testa F, Virga A, et al. MCM-41 functionalized with ethylenediaminetriacetic acid for ion-exchange chromatography. *Journal of Materials Chemistry*, 2011; 21(2): 369–376.
- [27] Chandrasekar G, You K S, Ahn J W, Ahn W S. Synthesis of hexagonal and cubic mesoporous silica using power plant bottom ash. *Microporous and Mesoporous Materials*. 2008; 111(1): 455–462.
- [28] Carvalho D L, de Avillez R R, Rodrigues M T, Borges L E, Appel L G. Mg and Al mixed oxides and the synthesis of *n*-butanol from ethanol. *Applied Catalysis A: General*, 2012; 415: 96–100.
- [29] Iatridis B, Gavalas G R. Pyrolysis of a precipitated kraft lignin. *Industrial & Engineering Chemistry Product Research and Development*, 1979; 18(2): 127–130.
- [30] Dorrestijn E, Laarhoven L J, Arends I W, Mulder P. The occurrence and reactivity of phenoxy linkages in lignin and low rank coal. *Journal of Analytical and Applied Pyrolysis*, 2000; 54(1): 153–192.
- [31] Foster A J, Jae J, Cheng Y T, Huber G W, Lobo R F. Optimizing the aromatic yield and distribution from catalytic fast pyrolysis of biomass over ZSM-5. *Applied Catalysis A: General*, 2012; 423: 154–161.
- [32] Idem R O, Katikaneni S P, Bakhshi N N. Catalytic conversion of canola oil to fuels and chemicals: roles of catalyst acidity, basicity and shape selectivity on product distribution. *Fuel Processing Technology*, 1997; 51(1): 101–125.
- [33] Carlson T R, Jae J, Lin Y C, Tompsett G A, Huber G W. Catalytic fast pyrolysis of glucose with HZSM-5: the combined homogeneous and heterogeneous reactions. *Journal of Catalysis*, 2010; 270(1): 110–124.
- [34] Li X, Su L, Wang Y, Yu Y, Wang C, Li X, et al. Catalytic fast pyrolysis of Kraft lignin with HZSM-5 zeolite for producing aromatic hydrocarbons. *Frontiers of Environmental Science & Engineering*, 2012; 6(3): 295–303.
- [35] Cheng Y T, Wang Z, Gilbert C J, Fan W, Huber G W. Production of *p*-Xylene from Biomass by Catalytic Fast Pyrolysis Using ZSM-5 Catalysts with Reduced Pore Openings. *Angewandte Chemie International Edition*, 2012; 51(44): 11097–110100.
- [36] Iliopoulou E, Antonakou E, Karakoulia S, Vasalos I, Lappas A, Triantafyllidis K. Catalytic conversion of biomass pyrolysis products by mesoporous materials: effect of steam stability and acidity of Al-MCM-41 catalysts. *Chemical Engineering Journal*, 2007; 134(1): 51–7.
- [37] Kaewpengkrow P, Atong D, Sricharoenchaikul V. Effect of Pd, Ru, Ni and ceramic supports on selective deoxygenation and hydrogenation of fast pyrolysis *Jatropha* residue vapors. *Renewable Energy*, 2014; 65: 92–101.
- [38] Kaewpengkrow P, Atong D, Sricharoenchaikul V. Catalytic upgrading of pyrolysis vapors from *Jatropha* wastes using alumina, zirconia and titania based catalysts. *Bioresource Technology*, 2014; 163: 262–269.
- [39] Auta M, Ern L, Hameed B. Fixed-bed catalytic and non-catalytic empty fruit bunch biomass pyrolysis. *Journal of Analytical and Applied Pyrolysis*, 2014; 107: 67–72.
- [40] Wang D, Xiao R, Zhang H, He G. Comparison of catalytic pyrolysis of biomass with MCM-41 and CaO catalysts by using TGA–FTIR analysis. *Journal of Analytical and Applied Pyrolysis*, 2010; 89(2): 171–177.